Electron-nucleus cusp correction and forces in quantum Monte Carlo

Manolo C. Per, Salvy P. Russo, and Ian K. Snook

Citation: The Journal of Chemical Physics **128**, 114106 (2008); doi: 10.1063/1.2890722
View online: http://dx.doi.org/10.1063/1.2890722
View Table of Contents: http://aip.scitation.org/toc/jcp/128/11
Published by the American Institute of Physics

Electron-nucleus cusp correction and forces in quantum Monte Carlo

Manolo C. Per,[a] Salvy P. Russo, and Ian K. Snook
Department of Applied Physics, School of Applied Sciences, RMIT University, Melbourne 3001, Australia

(Received 12 December 2007; accepted 11 February 2008; published online 19 March 2008)

A simple method is presented which ensures the electron-nucleus cusp condition is satisfied by the Slater-Jastrow wavefunctions commonly employed in quantum Monte Carlo simulations. The method is applied in variational energy calculations of the neon atom and a selection of molecules using both Gaussian and Slater basis sets. In addition, we discuss the relationship between the electron-nucleus cusps and the variance of forces, and investigate the sensitivity of forces to the quality of the cusps for various diatomic molecules. © *2008 American Institute of Physics*.
[DOI: 10.1063/1.2890722]

I. INTRODUCTION

Quantum Monte Carlo (QMC) methods are proving successful for calculating accurate properties of atomic, molecular, and solid state systems. The primary methods, namely, variational Monte Carlo (VMC) and diffusion Monte Carlo (DMC),[1] both require guiding trial wavefunctions. The accuracy of VMC results depend entirely on the quality of the trial wavefunction, while DMC is less sensitive, with only the nodal surface of the trial wavefunction affecting total energies. However, the statistical properties of both approaches, and the stability of DMC, depend on the accuracy of the trial wavefunction used.

When designing trial wavefunctions, it is sensible to include as many of the known properties of exact wavefunctions as possible. An advantage of Monte Carlo methods is that there are no restrictions on the form of the trial wavefunction, other than it must be computationally cheap to evaluate. Little is known about exact wavefunctions, but there are a number of general properties which can be made use of. The first is the antisymmetry of fermionic wavefunctions under particle exchange. This is efficiently incorporated into a many-body wavefunction using a product of spin-up and spin-down Slater determinants. The single-particle orbitals which make up the determinant are easily obtained from Hartree-Fock (HF) or density-functional calculations. Dynamic electron correlation effects can be included using a Jastrow factor, in which electron-electron distances appear explicitly. The resulting Slater-Jastrow trial wavefunction is a compact and efficient approximation to the true many-electron wavefunction,

$$\Psi_T = D^{\uparrow} D^{\downarrow} \exp(J). \tag{1}$$

The behavior of the exact wavefunction when two charged particles have a very small separation can be understood by rearranging the time-independent Schrödinger equation,

$$\epsilon = \frac{H\Psi}{\Psi} = \frac{\hat{T}\Psi}{\Psi} + V, \tag{2}$$

where ϵ is an eigenvalue of the Hamiltonian and Ψ is the corresponding eigenstate. As the eigenvalue is a constant, the divergence in the Coulomb potential which occurs as two charged particles coalesce must be countered by a corresponding divergence in the local kinetic energy $\Psi^{-1}\hat{T}\Psi$. The conditions on the wavefunction which ensure these divergences occur were derived by Kato in his formal study of the properties of exact wavefunctions.[2] Kato's cusp conditions are

$$\left.\frac{\partial(\Psi)_{\text{ave}}}{\partial r}\right|_{r=0} = \gamma\Psi(r=0), \tag{3}$$

where $(\Psi)_{\text{ave}}$ is the spherical average of the many-body wavefunction Ψ about the coalesence point, and r is the interparticle distance. For an electron-nucleus pair, $\gamma=-Z$ in atomic units, where Z is the charge of the nucleus.

The central quantity in QMC simulations is the local energy $E_L=\Psi_T^{-1}H\Psi_T$, which diverges near the nuclei if the cusp conditions are not met. This can increase the statistical error of QMC energies and cause instabilities in wavefunction optimization and DMC simulations. Previous work in this area has concentrated on the cusp correction of orbitals built from Gaussian basis functions. The work of Manten and Lüchow[3] showed that the primary cause of large variances in the local energy was the fluctuation of the second derivatives of the orbitals, a consequence of using many Gaussian basis functions. Their cusp correction method, while not imposing the exact cusp condition, significantly improves the quality of trial wavefunctions by removing these fluctuations. The more recent work of Ma *et al.*[4] goes further and shows how the exact cusp conditions may be enforced.

In this work, we present an alternative and simpler method for adding the exact electron-nucleus cusps to Slater-Jastrow trial wavefunctions. The new method has some similarities to that of Manten and Lüchow,[3] but our method imposes the exact cusp conditions and is easy to implement and automate. The cusp-correction method is tested on a set of molecules with trial wavefunctions built from both Gaussian

[a]Electronic mail: manolo.per@rmit.edu.au.

and Slater orbitals. In addition, we highlight the link between the electron-nucleus cusp conditions and the calculation of finite-variance forces in QMC. The cusp-correction method is used to investigate the sensitivity of forces to the quality of the cusp.

II. CUSP CORRECTION

For a Slater-Jastrow wavefunction, the electron-nucleus cusps can be built using the Slater determinant, the Jastrow factor, or both. Here we assume that the Jastrow factor contributes nothing to the cusp (i.e., $\partial J/\partial r|_{r=0}=0$), in which case the cusp condition becomes a set of conditions on the single-particle orbitals which make up the Slater determinant,

$$\left.\frac{\partial(\phi_i)_{\text{ave}}}{\partial r_A}\right|_{r_A=0} = -Z_A\phi_i(r_A=0) \quad \forall\, i,A. \tag{4}$$

Here i labels the orbital, and A the nucleus. For orbitals expanded in an atom-centered basis (such as Gaussian, Slater, numerical bases), only the s-type components of the basis functions centered on atom A will contribute to the cusp. The electron-nucleus cusp condition then becomes

$$\left.\frac{\partial\phi_i^{A,s}}{\partial r_A}\right|_{r_A=0} = -Z_A[\phi_i^{A,s}(r_A=0)+\eta_{iA}] \quad \forall\, i,A, \tag{5}$$

where η_{iA} is the contribution to the orbital ϕ_i at the position of nucleus A from basis functions centered on other nuclei. While the exact single-particle orbitals should obey the electron-nucleus cusp condition, those obtained from practical calculations rarely do.

A. Method

Our cusp correction method centers around the use of quintic splines[5,6] to represent the s-type parts of each orbital on each atom. A quintic spline is used rather than the more usual cubic spline so that the second and third derivatives of the orbital are smooth functions. The spline for a given orbital on a given atom is built using N_{knot} knots, with the ith knot placed at a radial distance proportional to $r_i=t_i/(1-t_i)$ where $t_i=(i-1)/N_{\text{knot}}$. This placement ensures that the knot density is higher closer to the nucleus, where the value of the orbital varies most rapidly. Far from the nucleus these knots sample the original s-type component of the orbital, but close to the nucleus we require the knots to sample a function with the correct cusp behavior. This is achieved by sampling a function of the following form:

$$f(r) = a\exp(-br)+cr+d. \tag{6}$$

The values of the parameters a,b,c,d are determined by performing a least-squares fit to the s-type part of the original orbital in the region close to the nucleus, under the constraint

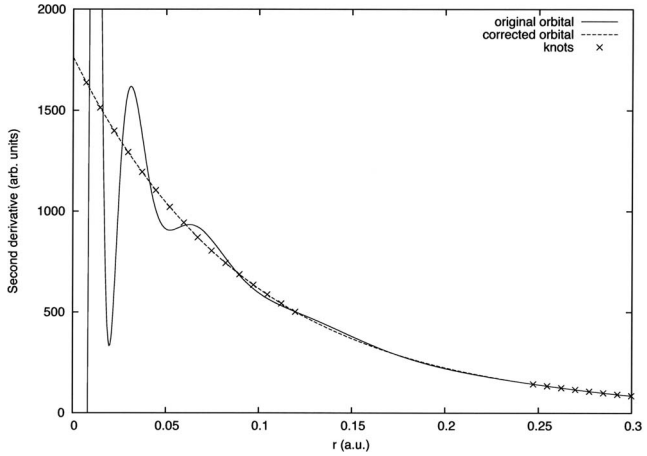

FIG. 1. The second derivative of the 1s orbital of Ne using a Gaussian 6-311G(d) basis. The knot void reaches from around 0.12 to 0.25 a.u.

$$d = \frac{ab-c}{Z} - a - \eta. \tag{7}$$

This ensures the function $f(r)$ obeys the cusp condition exactly. We find that a fit range of $[0,2/Z]$ works well, with the exception of hydrogen nuclei, for which we use $[0,1]$. A knot void is left between the two regions, so the join between the original orbital and the function $f(r)$ is spanned by a single quintic polynomial. A poor choice of the position and length of the knot void can cause large fluctuations in the derivatives of this polynomial. This is undesirable as it is the fluctuations in the second derivatives of the orbitals which lead to large variances in the local energy. A good choice produces a smooth join in the second derivative of the modified orbital, as shown in Fig. 1. The position and size of the knot void are chosen by requiring the third derivative of the spline at the left and right ends of the knot void to closely match the third derivatives of f and ϕ, respectively. This is achieved by minimizing the following cost function:

$$\chi = \left(\frac{\partial^3 S_- - \partial^3 f_-}{|\partial^2 f_-| + \delta}\right)^2 + \left(\frac{\partial^3 S_+ - \partial^3 \phi_+}{|\partial^2 \phi_+| + \delta}\right)^2. \tag{8}$$

Here we denote radial derivatives by $\partial^n = \partial^n/\partial r^n$, and S refers to the spline. A subscript $-/+$ indicates the value at the left/right edge of the knot void. A small constant δ is used to prevent the possibility of the cost function diverging. Simply choosing to minimize the difference in third derivatives would force the void region to values of large r, where the magnitudes of these values are smaller. The function χ takes advantage of the roughly exponential behavior of the ideal orbital to provide an r-independent cost function.

In order for the cusp condition to be satisfied exactly, it is essential that the spline is constrained such that the first derivatives at the knots are exactly the same as the function being sampled. This leads to a loss of continuity in the fourth derivative of the spline at the knots, but this is of no practical consequence. The routine we use to construct the quintic spline is QUINDF.[6]

While a large number of knots are initially used to construct the spline, we can easily resample and use a small number of knots for the final representation of the orbital. We

TABLE I. VMC energy and variance (σ^2) results using single-determinant trial wavefunctions. All quantities are in atomic units.

		VMC (no cusp correction)		VMC (with cusp correction)	
System	Hartree-Fock	Energy	σ^2	Energy	σ^2
Ne [G]	−128.523	−128.62(13)	3875(3670)	−128.5291(47)	33.13(54)
Ne [G-opt]	−128.547	−128.5524(81)	36(3)	−128.5493(41)	29.2(5)
LiH [G]	−7.9855	−7.9845(15)	8(2)	−7.98536(49)	1.607(16)
FH [G]	−100.033	−100.038(43)	677(367)	−100.0389(39)	26(2)
CH_3Cl [G]	−499.130	−499.18(10)	888(151)	−499.141(13)	136(1)
CH_3CH_2OH [G]	−154.110	−154.056(24)	269(53)	−154.1167(42)	36(1)
Li_2 [G]	−14.871	−14.8707(24)	13(1)	−14.87107(66)	3.127(69)
N_2 [G]	−108.961	−108.912(30)	276(76)	−108.9677(33)	24.76(46)
O_2 [G]	−149.647	−149.622(51)	533(185)	−149.6606(42)	33.9(5)
Si_2 [G]	−577.736	−577.673(90)	1426(464)	−577.7322(93)	155(2)
Ne [S]	···	−128.5268(51)	30.56(91)	−128.5298(48)	29.40(41)
LiH [S]	···	−7.98265(50)	1.589(26)	−7.98168(50)	1.533(15)
FH [S]	···	−100.0648(37)	22.34(28)	−100.0615(38)	22.22(38)
CH_3Cl [S]	···	−497.243(13)	156(2)	−497.238(14)	157(4)
CH_3CH_2OH [S]	···	−154.1393(40)	34.19(55)	−154.1314(39)	34.32(59)
Li_2 [S]	···	−14.871 59(67)	3.060(91)	−14.871 78(66)	3.034(51)
N_2 [S]	···	−108.9636(33)	23.55(25)	−108.9649(34)	23.58(42)
O_2 [S]	···	−149.6668(46)	34(2)	−149.6572(44)	32.6(4)
Si_2 [S]	···	−577.0883(89)	149(1)	−577.0901(92)	150(3)

find that 60 knots are perfectly adequate for representing the systems studied here. The use of a constant number of knots at fixed radial positions for all orbitals can improve the efficiency of the evaluation of the orbitals during a QMC simulation.

III. ENERGIES

In this section we apply the cusp correction method to a selection of molecules, with geometries taken from the G2 test set.[7] This selection includes methyl chloride (CH_3Cl) and ethanol (CH_3CH_2OH) along with a number of diatomic molecules.

For each molecule we compare the use of two different basis sets which were used to build the single-particle orbitals for the determinantal part of the trial wavefunction. The first basis set (labeled [G]) is the Gaussian 6-311G(d) basis, as implemented in the GAMESS code.[8] The second basis (labeled [S]) is the Slater TZP basis supplied with ADF.[9] We also consider the Ne atom using a very large optimized Gaussian basis set (labeled [G-opt]), in addition to the two basis sets already described. This even-tempered basis was optimized using the simplex method,[10] and consists of 20 *s*-type and 10 *p*-type functions. All the orbitals were generated using the HF method, and so are energy-optimal within each basis.

A. Energy results

Our implementation of the cusp correction method is automatic, and is well-behaved for all the systems we have studied. The results of VMC calculations on the test set are shown in Table I. The trial wavefunctions used for calculating VMC energies are single determinants built using the HF orbitals, so the VMC energies should agree with the HF energies, which are included for comparison where possible. For the Slater basis sets, there are no HF energies to compare with as the ADF code does not report total energies.

Occasionally the *s*-type part of an orbital will behave very differently to the ideal exponential-type form inside the fitting region. This is particularly true of orbitals which have a very small *s*-type component on a given nucleus, and occurs on the hydrogen nuclei in the ethanol molecule. However, the small magnitude of these *s*-type component means that even if the fit is relatively poor, there is no adverse effect on the total energy of the system. In addition, the join between the fitting function and the original *s*-type part of the orbital remains smooth.

All the cusp corrected energies agree well with the Hartree-Fock values, so there is no energy penalty to performing the cusp correction. The results show a very large reduction in the variance of the energy when using the cusp-corrected 6-311G(d) Gaussian basis sets. For the Ne atom, the non-cusp-corrected very large [G-opt] basis has a lower variance of the energy than that of the smaller [G] Gaussian basis set, even though the fluctuations of the second derivatives of the *s*-type orbitals are larger. This is because the fluctuations are closer to the nucleus, where by volume they contribute less. The effect of cusp correcting these orbitals is a minimal reduction in the variance. When using the Slater basis sets, there is practically no change in the variance or the value of the energy for any of the systems considered.

Overall, our results agree with the observation of Manten and Lüchow[3] that the main contribution to the variance of the energy is from the large fluctuations of the second derivatives of the orbitals, rather than the lack of the exact electron-nucleus cusp. The Slater basis sets used here are relatively small, but the use of larger Slater basis sets could exhibit these fluctuations, and so would benefit from cusp-correction.

IV. FORCES

The calculation of the forces on nuclei using QMC methods contains some well-known difficulties. In this section we review these difficulties and explain the role of the electron-nucleus cusp condition in obtaining forces with finite variance.

Force expressions in QMC can be obtained by directly differentiating the expectation value of the local energy. The z-component of the force on an atom labeled A is minus the derivative of the total energy with respect to the z-component of the position of that atom. In VMC we obtain

$$F_{Az}^{\mathrm{VMC}} = -\frac{\partial E_{\mathrm{VMC}}}{\partial R_{Az}} = -\left\langle \frac{\partial E_L}{\partial R_{Az}} \right\rangle - 2\,\mathrm{Cov}\left(E_L, \frac{1}{\Psi_T}\frac{\partial \Psi_T}{\partial R_{Az}}\right). \tag{9}$$

In DMC expectation values are taken over the distribution $\Psi_0\Psi_T$, where Ψ_0 is the exact ground-state wavefunction, and the force is

$$F_{Az}^{\mathrm{DMC}} = -\frac{\partial E_{\mathrm{DMC}}}{\partial R_{Az}} = -\left\langle \frac{\partial E_L}{\partial R_{Az}} \right\rangle - \mathrm{Cov}\left(E_L, \frac{1}{\Psi_T}\frac{\partial \Psi_T}{\partial R_{Az}}\right) - \mathrm{Cov}\left(E_L, \frac{1}{\Psi_0}\frac{\partial \Psi_0}{\partial R_{Az}}\right). \tag{10}$$

The expectation value of the derivative of the local energy is usually simplified, so that the force can be written in terms of the Hellmann-Feynman[11] expression and Pulay corrections.[12] In VMC, the expectation value of the derivative of the local kinetic energy vanishes, so the expectation value of the derivative of the local energy has the same value as the Hellmann-Feynman expression, and the force becomes

$$F_{Az}^{\mathrm{VMC}} = -\left\langle \frac{\partial V}{\partial R_{Az}} \right\rangle - 2\,\mathrm{Cov}\left(E_L, \frac{1}{\Psi_T}\frac{\partial \Psi_T}{\partial R_{Az}}\right). \tag{11}$$

In DMC, the expectation value of the derivative of the local kinetic energy does not vanish, but instead cancels one of the covariance terms, and we are left with

$$F_{Az}^{\mathrm{DMC}} = -\left\langle \frac{\partial V}{\partial R_{Az}} \right\rangle - \mathrm{Cov}\left(E_L, \frac{1}{\Psi_0}\frac{\partial \Psi_0}{\partial R_{Az}}\right) + N\left[\frac{\partial \Psi_T}{\partial R_{Az}}\right]. \tag{12}$$

The final term is a nodal term which accounts for the change in the approximate nodal surface with R_{Az}.[13]

The evaluation of the Hellmann-Feynman term is what causes problems in QMC. The derivative of the electron-nucleus interaction potential is

$$\frac{\partial V_{en}}{\partial R_{Az}} = -Z_A \sum_i \frac{(z_i - R_{Az})}{r_{iA}^3}, \tag{13}$$

which diverges as $1/r_{iA}^2$ as an electron approaches the nucleus, leading to an infinite variance.

One way to obtain forces with finite variance is to go back to Eqs. (9) and (10) and evaluate them directly. The presence of the derivative of the local energy in these expressions allows for the possibility of canceling the divergent derivative of the electron-nucleus potential using the derivative of the local kinetic energy. The origin of this cancellation can be seen by differentiating the local kinetic energy,

$$\frac{\partial}{\partial R_{Az}}\frac{\hat{T}\Psi_T}{\Psi_T} = \frac{1}{\Psi_T}\frac{\partial}{\partial R_{Az}}(\hat{T}\Psi_T) - \frac{\hat{T}\Psi_T}{\Psi_T}\frac{1}{\Psi_T}\frac{\partial \Psi_T}{\partial R_{Az}}. \tag{14}$$

The kinetic energy operator can be expanded in spherical coordinates about the atom A,

$$\hat{T}\Psi_T = -\frac{1}{2}\sum_i \nabla_i^2 \Psi_T = -\frac{1}{2}\sum_i \left[\frac{\partial^2 \Psi_T}{\partial r_{iA}^2} + \frac{2}{r_{iA}}\frac{\partial \Psi_T}{\partial r_{iA}} + \hat{L}_{iA}\Psi_T\right], \tag{15}$$

where we group the terms involving angular derivatives into $\hat{L}$, as only the spherical terms are relevant here. Now, the derivative of this expression is

$$\frac{\partial}{\partial R_{Az}}(\hat{T}\Psi_T) = -\frac{1}{2}\sum_i \left[\frac{\partial}{\partial R_{Az}}\left(\frac{\partial^2 \Psi_T}{\partial r_{iA}^2} + \hat{L}_{iA}\Psi_T\right) + \frac{2}{r_{iA}}\frac{\partial}{\partial R_{Az}}\frac{\partial \Psi_T}{\partial r_{iA}} + \frac{2(z_i - R_{Az})}{r_{iA}^3}\frac{\partial \Psi_T}{\partial r_{iA}}\right]. \tag{16}$$

From the final term, we can see that the first term in the derivative of the local kinetic energy [Eq. (14)] will contain the term

$$-\sum_i \frac{(z_i - R_{Az})}{r_{iA}^3}\frac{1}{\Psi_T}\frac{\partial \Psi_T}{\partial r_{iA}}. \tag{17}$$

If the trial wavefunction obeys the electron-nucleus cusp condition in Eq. (3), then close to the nucleus this term will exactly cancel the divergent derivative of the electron-nucleus potential, so a finite variance can be obtained.

There are three methods in the literature which have been proposed to enable the calculation of forces with finite variance. These are the s-wave filtering method of Chiesa *et al.*,[14] the correlated sampling method of Filippi and Umrigar,[15] and the renormalization method of Assaraf and Caffarel.[16]

The use of Eqs. (9) and (10) to calculate forces is equivalent to a special case of the zero-variance zero-bias extension[17] to Assaraf and Caffarel's original method, in which their auxillary function $\tilde{\psi}$ is chosen to be the derivative of the trial wavefunction. Although this approach should result in lower variance of the force than the original renormalization method, those authors found that this was not the case for the VMC force of the Li_2 molecule.[17] We attribute this to the lack of the exact electron-nucleus cusp in their trial wavefunction.

The correlated-sampling method can be used to obtain forces by calculating the energy difference between two closely related geometries. In this finite-difference correlated sampling (FDCS) approach, the VMC energy gradient is calculated as

TABLE II. Comparison of VMC forces calculated using the finite-difference correlated sampling approach. The same number of Monte Carlo samples are used for each result. All forces are in atomic units.

		No warp		With warp	
System	Hartree-Fock	No cusp correction	With cusp correction	No cusp correction	With cusp correction
LiH [G]	−0.00382	−0.25(38)	0.0010(65)	−0.003 22(69)	−0.00439(35)
Li_2 [G]	−0.00031	−0.38(39)	−0.0021(79)	0.000 87(51)	0.000 18(30)
N_2 [G]	0.18350	4(6)	0.179(61)	0.1825(83)	0.1815(32)
O_2 [G]	0.14993	−12(13)	0.228(92)	0.1429(90)	0.1475(38)
FH [G]	−0.04320	−44(42)	−0.23(10)	−0.000(28)	−0.0441(56)
LiH [S]	⋯	0.042(33)	−0.0096(63)	−0.002 78(31)	−0.002 62(32)
Li_2 [S]	⋯	−0.0116(82)	−0.0094(76)	−0.000 61(30)	−0.000 19(29)
N_2 [S]	⋯	0.21(14)	0.211(58)	0.1650(31)	0.1611(33)
O_2 [S]	⋯	0.09(13)	0.156(83)	0.1044(35)	0.1150(39)
FH [S]	⋯	−0.04(11)	−0.107(96)	−0.0327(51)	−0.0341(53)

$$\frac{\partial E}{\partial R_{Az}} = \frac{1}{\delta}\left[\frac{\langle wE_L(R_{Az}+\delta)\rangle}{\langle w\rangle} - \langle E_L(R_{Az})\rangle\right], \tag{18}$$

where the weights are $w=\Psi_T^2(R_{Az}+\delta)/\Psi_T^2(R_{Az})$ and δ is the displacement of the nucleus. The Monte Carlo samples are taken from the distribution $\Psi_T^2(R_{Az})$, with the *same* samples being used to calculate each expectation value. This method is also equivalent to using Eq. (9), with the fluctuations of the weights about unity performing the same role as the Pulay correction (the covariance term). Setting the weights to unity recovers the Hellmann-Feynman force.

A. Sensitivity of forces to cusp quality

It is reasonable to expect forces to be more sensitive to the quality of the electron-nucleus cusps than the energy, as the role of the cusp is to reduce the variance from a formally infinite value to a finite one. To test this sensitivity, we have compared the effect of using non-cusp-corrected wavefunctions and their cusp-corrected counterparts to evaluate the VMC force using the FDCS approach [Eq. (18)].

We also consider the effect of the space-warp transformation described by Filippi and Umrigar.[15] While the imposition of the electron-nucleus cusp condition results in forces with finite variance, this variance can still be rather large. The use of the space-warp transformation further reduces the variance. It works by moving the electrons close to a nucleus almost rigidly with that nucleus, so the electron distribution peaks at the position of the displaced nucleus.

B. Forces results

Forces for a selection of diatomic molecules are presented in Table II. For each molecule we use both Gaussian and Slater basis set HF determinants as the trial wavefunctions (labeled [G] and [S], respectively), so the VMC forces should agree with those obtained from HF calculations. The geometries are those given in the G2 test set[7] which were optimized at the MP2/6-31G(d) level, so the forces differ slightly from zero. We include the Hartree-Fock results only for the Gaussian based wavefunctions; as with the total energies, Hartree-Fock forces are not available in ADF.

The calculation of decorrelated statistics requires special care when calculating a ratio of two expectation values, as in Eq. (18). The use of a finite number of Monte Carlo samples to evaluate the ratio introduces a small systematic bias. When using the reblocking method,[18] the blocks must be large enough to obtain both decorrelated samples and reduce the bias in the ratio of expectation values to below statistical accuracy.

Without the space-warp, the results for the Gaussian based wavefunctions are meaningless without cusp correction, and the error bars can only be considered approximate. The corresponding results for the Slater based wavefunctions without cusp correction have much smaller errors than the Gaussians. Their variance is still technically infinite, but with a finite number of Monte Carlo samples the electrons rarely enter the divergent region. To illustrate this point, the individual samples of the Hellmann-Feynman component of the force for Li_2 are shown in Fig. 2. Without the cusp correction the samples show infrequent but very large spikes, but after cusp correction, the samples are much more uniform.

When the space-warp transformation is used, even the non-cusp-corrected Gaussian based wavefunctions produce good results, with errors smaller than the cusp-corrected forces without the space-warp. The reason for this is that

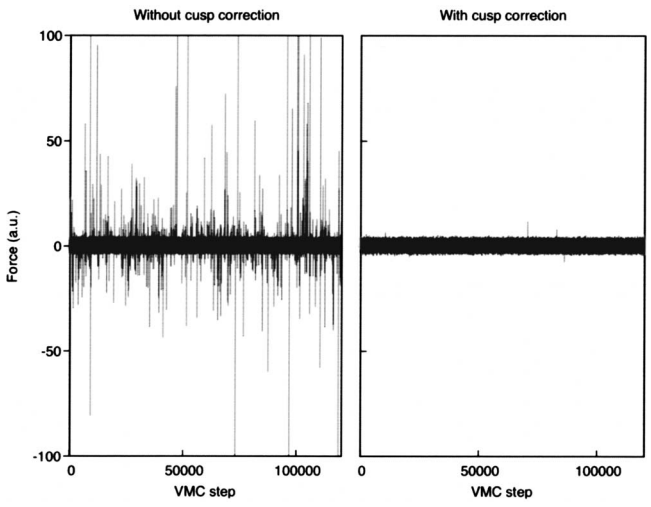

FIG. 2. Hellmann-Feynman component of the VMC force for the Li_2 molecule using cusp-corrected and non-cusp-corrected Slater basis functions. The trial wavefunction is a single Slater determinant.

when the nucleus is displaced, the space-warp causes those electrons closest to the nucleus (which are the ones responsible for the infinite variance) to move with it. The local energies sampled by these electrons are therefore very similar in the original and displaced geometries, and so their contribution to the force vanishes almost exactly. Using both the space-warp and the cusp-correction produces the most accurate results for the Gaussian based wavefunctions, with the benefit of cusp correction increasing with atomic number. For the Slater based wavefunctions, the quality of the results using the space-warp is unaffected by the cusp correction.

To summarize, the calculation of forces without the space-warp transformation is sensitive to the quality of the electron-nucleus cusp, with both Gaussian and Slater based trial wavefunctions showing smaller errors in the force after cusp correction. When the space-warp is used, only the Gaussian based wavefunctions benefit from the cusp correction. This implies the reason for the improvement is the reduction in the fluctuations of the second derivatives of the orbitals. We expect the same pattern of results to apply for forces calculated within DMC.

V. CONCLUSION

We have presented a simple and easily implementable method for ensuring the single-particle orbitals used in quantum Monte Carlo trial wavefunctions exactly obey Kato's electron-nucleus cusp conditions. The method has been applied to a number of molecules using both Gaussian and Slater basis sets where it proves robust and effective.

We have also discussed the calculation of forces with finite variance, and have used the cusp correction method to investigate the sensitivity of forces calculated using the finite-difference correlated sampling approach to the quality of the electron-nucleus cusp. The results of this investigation show that the space-warp electronic coordinate transformation is important in reducing the sensitivity of forces to the quality of the cusp. Forces calculated with the space-warp technique using Gaussian based wavefunctions show considerably reduced errors after cusp correction.

ACKNOWLEDGMENTS

We thank Garry Keltie and the RMIT Virtual Reality Centre for the use of their SGI Altix computer. This work was supported by the Australian Research Council (ARC), the Australian Partnership for Advanced Computing (APAC), and the Victorian Partnership for Advanced Computing (VPAC).

[1] W. M. C. Foulkes, L. Mitas, R. J. Needs, and G. Rajagopal, Rev. Mod. Phys. **73**, 33 (2001).
[2] T. Kato, Commun. Pure Appl. Math. **10**, 151 (1957).
[3] S. Manten and A. Lüchow, J. Chem. Phys. **115**, 5362 (2001).
[4] A. Ma, M. D. Towler, N. D. Drummond, and R. J. Needs, J. Chem. Phys. **122**, 224322 (2005).
[5] J. G. Herriot and C. H. Reinsch, ACM Trans. Math. Softw. **2**, 281 (1978).
[6] J. G. Herriot and C. H. Reinsch, ACM Trans. Math. Softw. **9**, 258 (1983).
[7] L. A. Curtiss, K. Raghavachari, P. Redfern, and J. A. Pople, J. Chem. Phys. **106**, 1063 (1997).
[8] M. W. Schmidt, K. K. Baldridge, J. A. Boatz, S. T. Elbert, M. S. Gordon, J. H. Jensen, S. Koseki, N. Matsunaga, K. A. Nguyen, S. Su, T. L. Windus, M. Dupuis, and J. A. Montgomery, Jr., J. Comput. Chem. **14**, 1347 (1993).
[9] G. te Velde, F. N. Bickelhaupt, E. J. Baerends, C. Fonseca Guerra, S. J. A. van Gisbergen, J. G. Snijders, and T. Ziegler, J. Comput. Chem. **22**, 931 (2001).
[10] W. H. Press, B. P. Flannery, S. A. Teukolsky, and W. T. Vetterling, *Numerical Recipes in Fortran: The Art of Scientific Computing*, 2nd ed. (Cambridge University Press, Cambridge, 1992).
[11] R. P. Feynman, Phys. Rev. **56**, 340 (1939).
[12] P. Pulay, Mol. Phys. **17**, 197 (1969).
[13] K. C. Huang, R. J. Needs, and G. Rajagopal, J. Chem. Phys. **112**, 4419 (1999).
[14] S. Chiesa, D. M. Ceperley, and S. Zhang, Phys. Rev. Lett. **94**, 036404 (2005).
[15] C. Filippi and C. J. Umrigar, Phys. Rev. B **61**, R16291 (2000).
[16] R. Assaraf and M. Caffarel, J. Chem. Phys. **113**, 4028 (2000).
[17] R. Assaraf and M. Caffarel, J. Chem. Phys. **119**, 10536 (2003).
[18] H. Flyvberg and H. Peterson, J. Chem. Phys. **91**, 461 (1989).